Manuscript prepared for Atmos. Meas. Tech.
with version 3.2 of the LaTeX class copernicus.cls.
Date: 13 February 2012

NO_2 Measurements in Hong Kong using LED Based Long Path Differential Optical Absorption Spectroscopy

K.L. Chan[1], D. Pöhler[2], G. Kuhlmann[1], A. Hartl[1], U. Platt[2], and M.O. Wenig[1]

[1]School of Energy and Environment, City University of Hong Kong
[2]Institute for Environmental Physics, Heidelberg University

Correspondence to: K.L. Chan
(kalokchan7@student.cityu.edu.hk)

Abstract. In this study we present the first long term measurements of atmospheric nitrogen dioxide (NO_2) using a LED based Long Path Differential Optical Absorption Spectroscopy (LP-DOAS) instrument. This instrument is measuring continuously in Hong Kong since December 2009, first in a setup with a 550 m absorption path and then with a 3820 m path at about 30m to 50 m above street level. The instrument is using a high power blue light LED with peak intensity at 450 nm coupled into the telescope using a Y-fibre bundle. The LP-DOAS instrument measures NO_2 levels in the Kowloon Tong and Mongkok district of Hong Kong and we compare the measurement results to mixing ratios reported by monitoring stations operated by the Hong Kong Environmental Protection Department in that area. Hourly averages of coinciding measurements are in reasonable agreement (R=0.74). Furthermore, we used the long-term data set to validate the Ozone Monitoring Instrument (OMI) NO_2 data product. Monthly averaged LP-DOAS and OMI measurements correlate well (R=0.84) when comparing the data for the OMI overpass time. We analyzed weekly patterns in both data sets and found that the LP-DOAS detects a clear weekly cycle with a reduction on weekends during rush hour peaks, whereas OMI is not able to observe this weekly cycle due to its fix overpass time (13:30 - 14:30 local time).

1 Introduction

Nitrogen dioxide (NO_2) is one of the most important trace gases in the atmosphere with impact on atmospheric chemical processes and public health. Nitrogen oxides (NO_x), defined as the sum of nitrogen oxide (NO) and nitrogen dioxide (NO_2), participate in the catalytic formation of ozone (O_3) in the troposphere. Acid rain caused by NO_x is known to have adverse impact on forest, freshwater

and soil, harming insects and aquatic life-forms, as well as causing damage to buildings and having a negative impact on public health. NO_2 may also play an important role in radiative warming of the earth's atmosphere (Solomon et al., 1999). Besides natural sources and biomass burning, fossil fuel combustion is estimated to contribute about 50 % to the global NO_x emission (Lee et al., 1997). In Hong Kong, the atmospheric NO_2 levels are strongly related to traffic volume (Lau et al., 2008) and power generation. Due to prevailing easterlies in Hong Kong, most of the power plants are built in the western part of Hong Kong to minimize the impact on the populated area. As in most metropolitan areas the NO_2 level varies rapidly with time. Having an accurate NO_2 measurement with high temporal resolution is very important for air quality monitoring and pollution management.

Differential Optical Absorption Spectroscopy (DOAS), introduced by Platt et al. (1979), is a spectroscopic measurement technique which has been used successfully for decades for atmospheric trace gas retrieval. DOAS allows direct and sensitive detection of multiple trace gases simultaneously without influencing their chemical interactions. It uses distinct narrow band absorption structures of the different trace gases for quantitative detection and concentration estimation by separating them from the broad band parts caused mainly by atmospheric scattering and broad band absorption.

In this paper, details of our experimental setup of the LED based fibre long path DOAS instrument are presented. The data are automatically analyzed for NO_2 and published on our website in near real time (airquality.e2.cityu.edu.hk/Data). The LP-DOAS NO_2 measurements are compared to the mixing ratios measured by a nearby monitoring station which is operated by the Hong Kong Environmental Protection Department (EPD), as well as the NO_2 data measured by the Ozone Monitoring Instrument (OMI) on board NASA's Aura satellite.

2 Experimental Setup and Retrieval Procedure

A sketch of the fibre LP-DOAS instrument setup is shown in Figure 1. The LP-DOAS setup consists of a blue LED light source, a telescope acting as sending and receiving unit and an array of retro reflectors (7 single quartz glass prisms each 63 mm in diameter) at the other end of the absorption path. Following the approach by Merten et al. (2011), the optical fibers were used as transmitter for the light between light source and telescope and telescope and spectrograph, respectively. The fibers are connected in a Y-bundle (5 m length) with six 200 μm transmitting fibers (NA=0.22) from the LED light source surrounding one 200 μm receiving fiber which is connected to the spectrometer. The high power LED is placed on a heat sink in order to stabilize the temperature. The light of the high power blue LED (CREE XR-E 7090 royal blue, 440-455 nm FWHM) with $\sim$600 mW radiant flux (at 700 mA) is collimated into the six fibres by a quartz glass lens with f=25 mm. The combined Y-fiber end is placed close to the focal point of the telescope's main mirror of 20 cm diameter and 60 cm focal length and thus produces an almost parallel light beam. Two stepper motors allow precise adjustment of the telescope to the retro reflector array. Light coming back from the retro

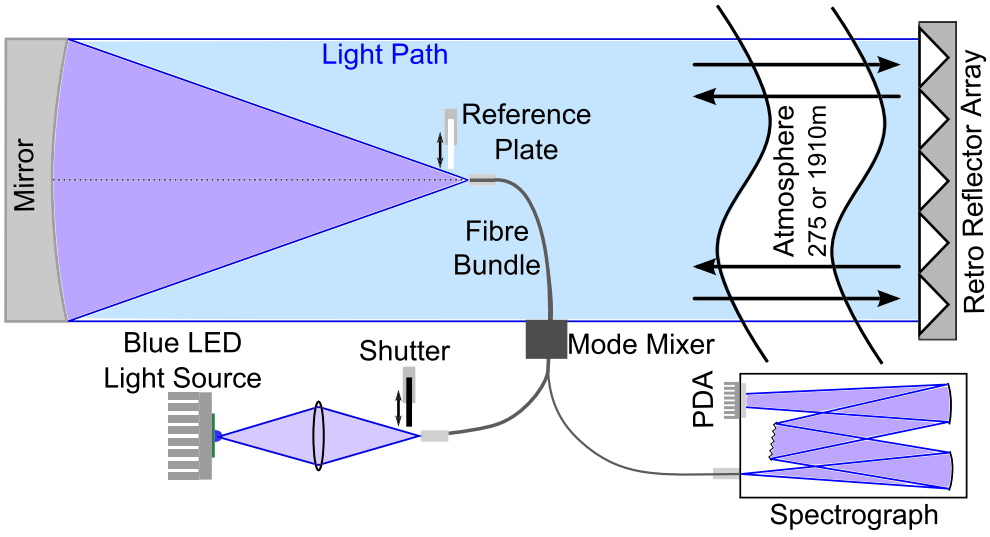

Fig. 1. Schematic diagram of the experimental setup of the fibre LP-DOAS.

reflector array is collected by the receiving fibre and redirected to a Triax 320 spectrometer (Jobin Yvon, f-number=4.0, 1200 l/mm grating and blaze 500 nm, f=320 mm, wavelength range from 400 to 462 nm, thermostated to 30°C). The detector is a HMT (Hoffmann Messtechnik) 1024 pixel photodiode array detector (with Hamamatsu S3904-1024 chip) temperature stabilized to 0°C. The 200 μm fibre acts as entrance slit, resulting in a spectral resolution of 0.4 nm (FWHM). To guarantee a homogeneous illumination of the spectrometer a mode mixer is applied by bending and vibrating the fibre (Stutz and Platt, 1997).

In this study, two measurement setups were realized (see Figure 2). Setup 1 was operational from December 2009 till November 2010 with a total absorption path of 550 m across the City University of Hong Kong (CityU) campus. Both the instrument and the reflector were located on top of university buildings at opposite ends of the campus. Setup 2 is operational since December 2010 with a total absorption path of 3820 m. The instrument is located at CityU and the retro reflector is installed at the 22^{nd} floor of the Langham Place Hotel at 70 m height in the center of Kowloon in Mong Kok. The measurement path covers the University campus, residential areas and areas with heavy traffic.

A measurement sequence starts with taking an atmospheric spectrum with a maximum of 10 scans followed by 10 scans of the LED reference spectrum. One scan is a spectrum with peak intensity about 60 % saturation of the detector and typically requires 60 ms to 1000 ms depending on visibility and instrument setup. The total sampling time for 10 scans is limited to 30 s, if longer scans are necessary, the number of scans is reduced. The LED reference spectrum is taken by using

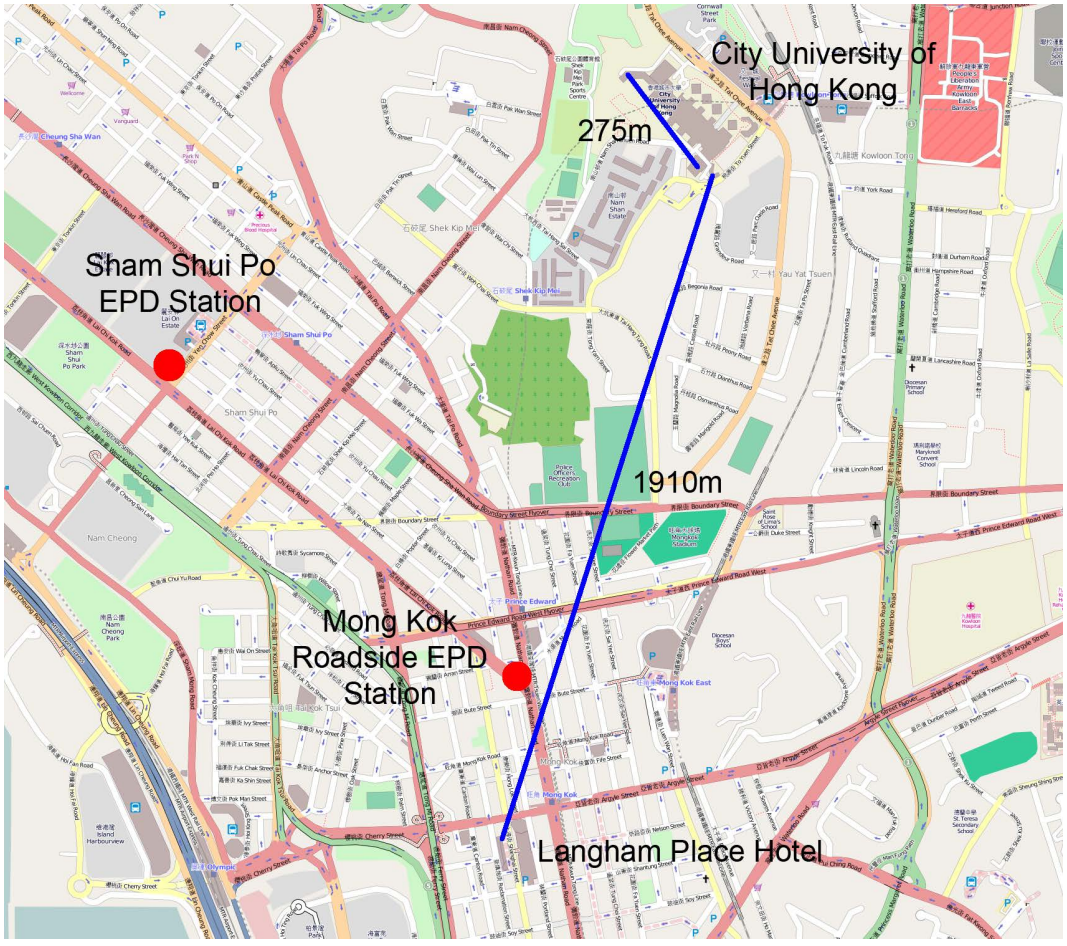

Fig. 2. Map of Kowloon, Hong Kong, from Open Street Map (http://www.openstreetmap.org) . The two blue lines indicate the measuring path for the two setups. The two red markers indicate the location of the Shum Shui Po and Mongkok EPD monitoring station.

a shortcut system consisting of an aluminum diffuser plate that is moved several millimeters in front of the fibre bundle, the measurement of the LED spectrum normally take less than 1 s. The narrow band structures of the LED reference spectra are used to account for changes in the detector and the LED itself in order to improve the quality of the DOAS fit. Afterwards an atmospheric background spectrum is taken by blocking the LED using a shutter with a fixed integration time of 1 s and 1 scan. A full measurement sequence takes between 30 s and 60 s depending on visibility conditions. For the LP-DOAS measurement and data evaluation the software DOASIS (Kraus, 2005) (doasis.iup.uni-heidelberg.de) is used.

The calibration of the spectrograph is performed using the emission lines of a Mercury lamp and a Xenon glow lamp. The Mercury emission line at 435.84 nm is used to convolve the literature reference spectra to the instrument resolution. The measured data are evaluated by the DOASIS

software. All spectra are corrected for offset, dark current and background before the DOAS fit. The measurement spectrum is then divided by the corresponding LED reference spectrum before taking the logarithm. In order to remove the broad band structures from the spectrum, a high pass filter is applied by subtracting a binomial filter of the order of 1000, corresponding to Gaussian smoothing with $\sigma = 22$ (in channels). Remaining broad band structures are removed by fitting and subtracting a second order polynomial during the DOAS fit.

In order to correct for small uncertainties in the wavelength mapping, we use one set of shift and squeeze parameters for all references spectra. The latter are taken from: NO_2 (Voigt et al., 2002), Glyoxal (CHOCHO) (Volkamer et al., 2005), O_3 (Voigt et al., 2001), O_4 (Greenblatt et al., 1990) and H_2O (Hitran 2006, see Rothman et al., 2003). For the non-linear optimization DOASIS uses a Levenberg-Marquard fit and b-splines for interpolation. The reference spectra are treated with the same high pass filter as applied for the measurement spectra. The spectral fit is performed in the wavelengths from 436.3 nm to 460.5 nm which includes several strong NO_2 absorption lines. The measured slant columns are converted to mixing ratios by dividing the slant columns by the total absorption length and the air density. Simultaneous pressure and temperature measurements are used for the air density calculation. A DOAS fit example of the LP-DOAS measurement is shown in Figure 3 with NO_2 slant column density of $1.84\times10^{17} \pm 1.53\times10^{15}$ molec/cm^2 with respect to volume mixing ratio of 19.23 ± 0.16 ppbv. Based on findings by Stutz and Platt (1996) the numerical error of the fit is multiplied by a factor of 3 to obtain an estimate of the measurement error (1σ) which is typically about 0.3 ppbv. The detection limit is defined by 2 times this measurement error (Stutz and Platt, 1996). We compared this detection limit to an estimate gained from analyzing the higher frequency variations in our time series. The latter are assumed to be dominated by instrument noise as path averaged NO_2 columns should vary on larger time scales. Applying a high pass filter with a threshold of 10 minutes to the data of one day, we obtain a variance of the remaining high frequency structure of about 0.5 ppbv, which agrees well with the estimate of the measurement error from the DOAS evaluation. This value is considered to be the upper limit of the measurement error. Typically, the error of the NO_2 measurement is in the order of 1 % and thus ignoreable in the following discussions. The LP-DOAS measurement error is not plotted in the comparison time series, since they are too small to be visible.

3 Results

The LP-DOAS has been measuring for more than 16 months, providing atmospheric NO_2 information with high temporal resolution. The data show strong daily, weekly and seasonal variability with lower NO_2 levels in summer and higher values in autumn and winter. Mean daily cycles of NO_2 for weekdays and Sunday show different characteristics. The typical daily cycle of NO_2 in an urban area shows one peak in the morning and one peak in the evening rush hour. The lowest and highest

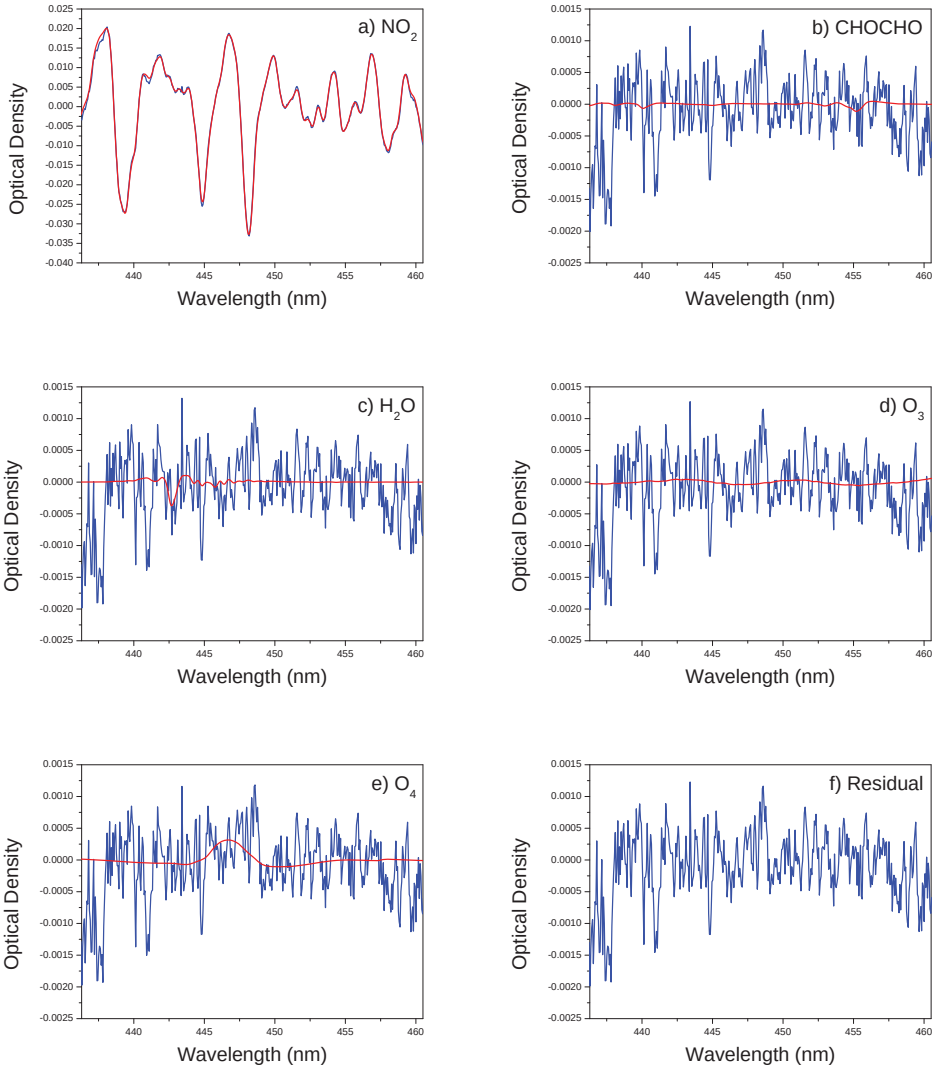

Fig. 3. Example of the NO_2 retrieval form a spectrum taken on 17 December 2010 at 09:54 (HKT). The optical density of the scaled cross-sections (red curves) and the sum of the scaled cross-section and the residual (blue curves) of (**a**) NO_2, (**b**) CHOCHO, (**c**) H_2O, (**d**) O_3 and (**e**) O_4. (**f**) shows the residual.

NO_2 levels usually occur in the early morning and the evening rush hour, respectively. Details of the daily and weekly cycle of NO_2 will be discussed in section 3.3. The annually averaged NO_2 mixing ratio measured by the LP-DOAS is about 23.5 ppbv, which is slightly higher than the WHO guideline annual value (21 ppbv), but considerably lower than the Hong Kong air quality annual objective value (42.5 ppbv). The maximum and minimum NO_2 mixing ratio measured within the entire measuring period are 110.9 ppbv and 2.6 ppbv, respectively.

During this study, we also analyzed the relationship between NO_2 mixing ratios, wind direction and wind speed. In general, the NO_2 mixing ratio is slightly higher when there are westerly winds, most likely due to transport from Hong Kong power plants. We could not observe a clear relation for wind from the industrial area in the Pearl River Delta NW of Hong Kong. This indicates that high NO_2 levels in Hong Kong do not arise from transport from these areas but have a local origin. We also find that the NO_2 levels decrease with increasing wind speed for all wind directions. Stronger winds prevent locally produced NO_2 from accumulating.

3.1 Comparison with In-situ Monitoring Data

In this section, we compare NO_2 measurements between the LP-DOAS and a nearby air quality monitoring station operated by the Hong Kong Environmental Protection Department (EPD) in Sham Shui Po about 1.6 km from our measuring site (www.epd-asg.gov.hk/english/backgd/quality.html). The monitoring station is located on top of the Sham Shui Po police station at about 17 meters above ground. The monitoring instrument is a chemiluminescence analyzer with a Molybdenum converter which measures atmospheric NO_2 by converting NO_2 to NO. Roadside measurements of another EPD station with the same type of instrument located in Mongkok are given in the following as well. The location of both EPD stations are marked in Figure 2.

Time series of daily averaged ambient NO_2 mixing ratios obtained by the LP-DOAS and the EPD monitoring station from December 2009 till March 2011 are shown in Figure 4a. Figure 4b and c show the EPD measurements and hourly averaged LP-DOAS measurements for the two setups, respectively. For setup 2 data from the EPD roadside monitoring station in Mongkok are also shown. NO_2 levels show similar characteristic: Both time series show a pronounced daily and annual cycle with lower NO_2 levels in summer. Ground level NO_2 in urban area is generally lower in summer due to a shorter NO_2 lifetime.

Figure 5a shows that the Pearson correlation coefficient between the CityU LP-DOAS and Sham Shui Po EPD data set is 0.71, the total error weighted least square regression has a slope of 0.81 with an offset of 16.01 ppbv. On average the EPD monitor in Shum Shui Po measures mixing ratios that are 11.5 ppbv higher than the LP-DOAS. This might be explained by the difference in the environment of the measuring sites. The EPD monitoring station is located in Sham Shui Po, a commercial area with heavy traffic, while the LP-DOAS instrument was set up in Kowloon Tong with the absorption path covering the University Campus and residential area.

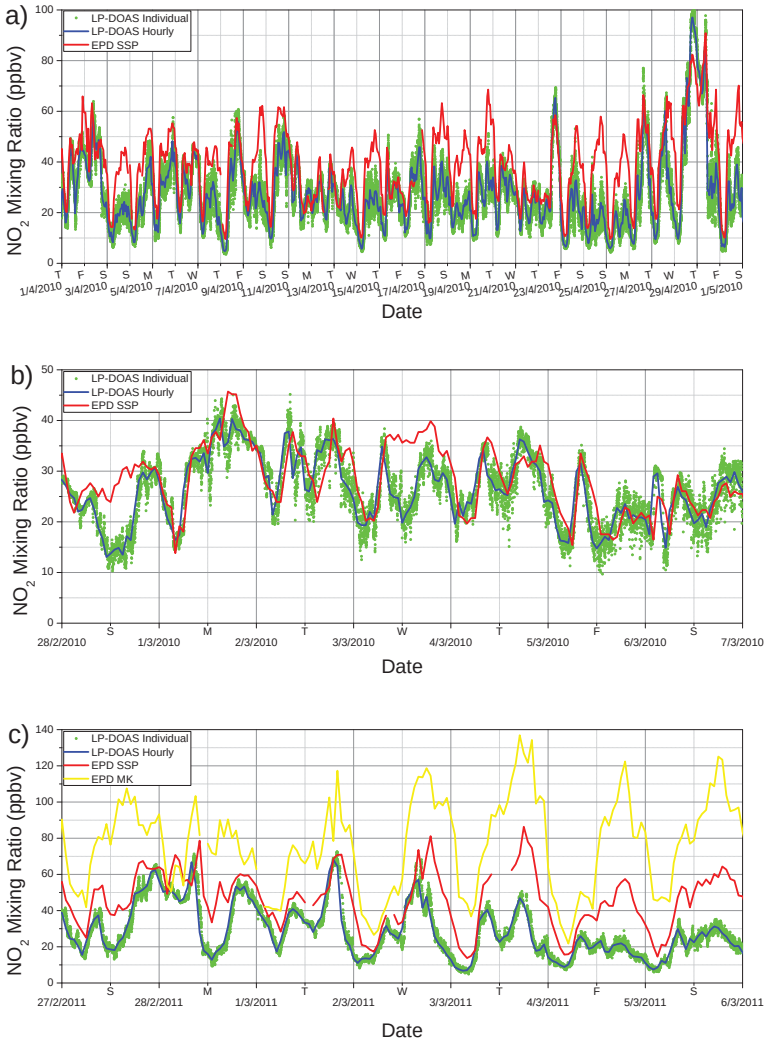

Fig. 4. Atmospheric NO_2 mixing ratio measured by LP-DOAS at CityU, EPD Sham Shui Po (SSP) and Mong Kok (MK) monitoring station. (**a**) Daily averaged data from December 2009 to March 2011, (**b**) and (**c**) NO_2 time series for the first week of March of 2010 and 2011, respectively.

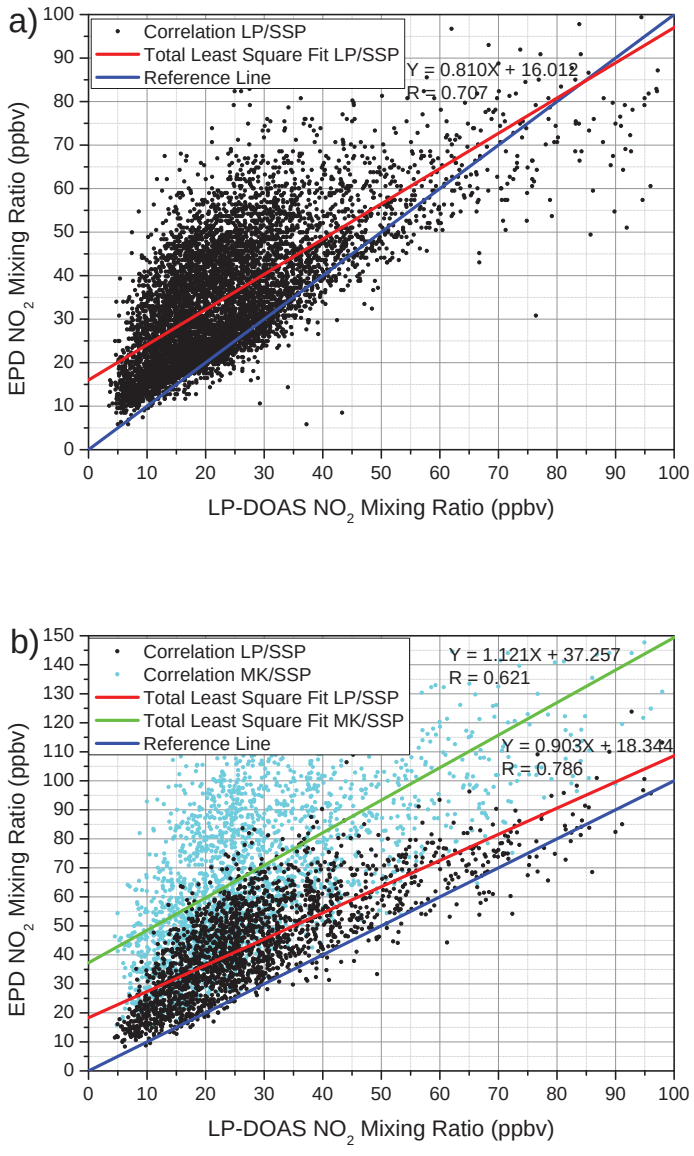

Fig. 5. (**a**) Correlation between mixing ratios measured by the LP-DOAS (LP) with CityU path (setup 1, 550 m path) and the EPD Sham Shui Po (SSP) monitoring station, for data from December 2009 to November 2010. (**b**) Correlation between mixing ratios measured by the LP-DOAS (LP) with Langham Place path (setup 2, 3820 m path) and the EPD Sham Shui Po (SSP, black dots) and Mongkok (MK, cyan dots) monitoring station, for data from December 2010 to March 2011.

The Pearson correlation coefficient between the LP-DOAS with path from CityU to Langham Place Hotel and EPD measurements in Sham Shui Po is 0.79, decreasing to 0.62 for the correlation between the LP-DOAS and Mongkok EPD roadside measurements, see Figure 5b. On average the Sham Shui Po and Mongkok EPD values are 15.6 ppbv and 40.7 ppbv higher than the LP-DOAS. Measured mixing ratios decreasing with increasing measurement height suggesting that the main emission sources and formation of NO_2 are very close to the ground and probably dominated by traffic emissions. This result agrees with the observation that the EPD roadside monitoring stations typically measure higher NO_2 levels than the average station (Lau et al., 2008).

Figure 4 illustrates that most of the time the NO_2 mixing ratios recorded by the EPD monitoring station correlate well with the LP-DOAS measurements. However, the EPD monitoring station measurements occasionally show a considerable disagreement compared to the LP-DOAS measurements (e.g. Figure 4b, 28 February and 3 March, 2010). This phenomenon may arise from the fact that emissions at the street level could be trapped by an inversion and cannot reach the height of the LP-DOAS. The discrepancy can also be explained by the differences in the measuring technique. The LP-DOAS remote sensing measures atmospheric NO_2 without any cross sensitivity to other nitrogen species, whereas the chemiluminescence analyzing technique is reported to suffer from significant interference by other nitrogen compounds. The conversion of these compounds can lead to overestimation of the measured NO_2 level up to 50 % in heavily polluted urban areas like Hong Kong (Dunlea et al., 2007). Additionally, the chemiluminescence measurement is a point measurement, while the LP-DOAS measures the average NO_2 mixing ratio along an absorption path. Therefore, the LP-DOAS is less influenced by a single emission source and local fluctuations.

3.2 Satellite Measurement Validation

Satellite measurements of atmospheric trace gases are indispensable for providing global maps of trace gas distributions. However, there are very few satellite validation studies over South China. In order to find out how representative satellite derived NO_2 columns are for ground level mixing ratios in Hong Kong, we compare the LP-DOAS NO_2 data to OMI satellite measurements.

3.2.1 The Ozone Monitoring Instrument

OMI is an imaging spectrometer measuring atmospheric trace gases such as NO_2 and O_3 (Levelt et al., 2006). It is on board the Earth Observing System's (EOS) Aura satellite which was launched on 15 July 2004 and is collecting data since 9 August 2004, providing more than 6 years of daily global NO_2 maps (Boersma et al., 2001). The Aura satellite orbits at an altitude of 705 km are in a sun-synchronous polar orbit with an exact 16 day repeat cycle and a local equator crossing time of 13:45 (local time) on the ascending node. The instrument consists of two nadir viewing imaging spectrometers measuring the UV/VIS spectral range from 264 nm to 504 nm with a spectral resolution between 0.45 nm and 1.0 nm FWHM. The spectral sampling is two to three times the

spectral resolution. OMI provides measurements at 60 positions across the orbital track every 2 seconds. In the global observation mode, these 60 measurements cover a swath of approximately 2600 km. The ground pixel size of OMI at nadir is about 320 km^2 (13 km $\times$ 24 km) and increases to about 6400 km^2 (40 km $\times$ 160 km) at the two ends of the track. The change in ground pixel size, and hence spatial resolution, must be taken into account when analyzing and interpreting OMI data. A more detailed description of the OMI instrument can be found in Levelt et al. (2006).

3.2.2 OMI Tropospheric NO_2 VCD Retrieval

In this study, NASA's OMI tropospheric NO_2 data product is used (Bucsela et al., 2006). The NO_2 slant column density (SCD) is retrieved by fitting the OMI spectrum for wavelengths ranging from 405 nm to 465 nm using the DOAS technique. For the OMI NO_2 data product three trace gas reference spectra, NO_2 (Vandaele et al., 1998), O_3 (Burrows et al., 1999) and H_2O (Harder and Brault, 1997), are fitted to the measured spectra. The air-mass factor (AMF), defined as the ratio of the SCD to the vertical column density (VCD), is needed in order to convert SCD into VCD (Solomon et al., 1987). The AMF calculation depends on the viewing geometry, surface albedo, atmospheric scattering and the NO_2 vertical profile (Palmer et al., 2001). AMFs are calculated on the basis of annual mean NO_2 profiles obtained from the GEOS-Chem model (Bey et al., 2001) and pre-calculated altitude-dependent AMFs (Bucsela et al., 2006). The stratospheric and tropospheric amounts of NO_2 are separated by assuming the tropospheric NO_2 varies on a much smaller spatial scale than the stratospheric NO_2. Polluted regions are masked and the remaining stratospheric field is smoothed and interpolated using a zonal planetary wave analysis. This smoothed field is subtracted from the VCDs in order to calculate the tropospheric NO_2 amount by applying a corrected tropospheric AMF. For cloud contaminated pixels profiles are extrapolated to the ground (Bucsela et al., 2006).

3.2.3 Gridded OMI NO_2 Data

Since there might be multiple OMI pixels overlapping each other, the OMI tropospheric NO_2 VCDs are gridded onto a high resolution longitude-latitude grid, in order to have a better comparison between the OMI NO_2 and the LP-DOAS measurements. For the comparison a $0.02^\circ \times 0.02^\circ$ grid (approximately 2.22 km $\times$ 2.05 km for Hong Kong) is used. The gridded product is based on all VCDs observed within a day for cloud cover less than 40 %. For overlapping OMI pixels a weighted average is stored in the grid cell. Weighting the VCDs with a factor $1/\mathrm{VCD}_{err}^2$ would minimize the resulting average errors. However, the AMF calculation constitutes the largest error source, which leads to the NO_2 VCD uncertainties being proportional to the VCDs. Weighting with $1/\mathrm{VCD}_{err}^2$ yields an average bias toward low VCD values. Following the approach introduced by Wenig et al. (2008), we adopt a weighting scheme which only depends on the error caused by the cloud cover C

and the OMI pixel size A for the calculation of VCD_{GRID}

$$VCD_{GRID} = \frac{\Sigma VCD \times W}{\Sigma W} \text{ with } W = \frac{1}{A(1.5 \times 10^{15}(1+3C))^2} \quad (1)$$

This gridding scheme can also enhance the details in the gridded product by giving smaller OMI pixels higher weights (Wenig et al., 2008).

3.2.4 Converting Tropospheric VCD to Ground Level Mixing Ratio

The OMI tropospheric NO_2 VCDs are converted to ground level mixing ratios using the OMI a-priori vertical NO_2 profile which is an annually averaged tropospheric profile from September 1996 to August 1997 derived from a global 3-D chemical transport model (CTM) GEOS-Chem (Bey et al., 2001). The profile used to convert OMI NO_2 VCDs to ground mixing ratios is shown in Figure 6. An annual mean (from July 2009 to June 2010), winter (December, January and February) and summer (June, July and August) vertical NO_2 profiles from GEOS-Chem are also shown and used for comparison.

3.2.5 Cloud Filtering

Clouds shield ground level NO_2 and make satellite measurements difficult. In order to allow better comparison with the LP-DOAS data, OMI measurements significantly influenced by clouds have to be filtered out. To get a balance between having enough measurements left and minimizing cloud contamination, only OMI data with cloud fractions smaller than 40 % are used in this study. LP-DOAS data from 13:30 to 14:30 local time (which is the OMI overpass time for Hong Kong and hence is expected to have the best agreement with OMI data) are used for comparison with the gridded OMI data sets within 15 km from the measurement site (which is approximately the average OMI pixel size), see Figure 7. OMI data within 50 km are shown for illustrations as well. In order to reduce the influence of clouds and local spatial variations, monthly mean data are used for the comparison.

3.2.6 Comparison of Monthly Values

Figure 8 shows the monthly averaged LP-DOAS data for the OMI overpass time from 13:30 to 14:30 and the OMI data converted to ground mixing ratios within a 15 km radius of CityU. Both data sets (LP-DOAS and OMI) show a very similar annual cycle with lower NO_2 values in summer and higher NO_2 values in autumn and winter. The Pearson correlation between the monthly means of LP-DOAS measurements and OMI data within 15 km is 0.84. In order to show the influence of temporal averaging, monthly averages for all LP-DOAS data are shown in Figure 8, too. As NO_2 shows high temporal variability, increasing the averaging time would include data that OMI is not able to capture and hence less correlated with each other. OMI data averaged for a 50 km radius illustrates the influence of spatial averaging. As can be seen in Figure 7, Hong Kong is at the edge

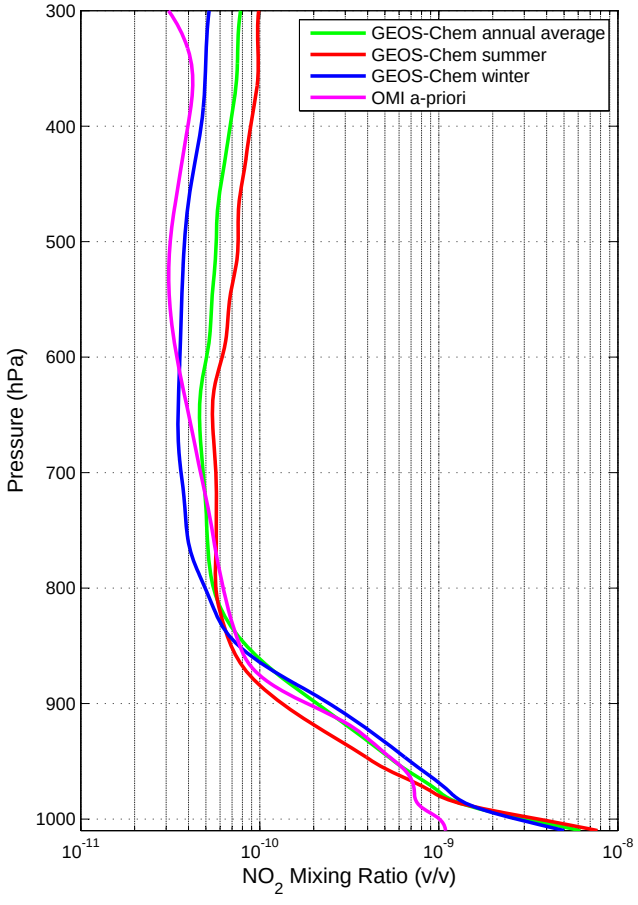

Fig. 6. Vertical profile of NO_2 for VCDs to ground level mixing ratio conversion. The green, red and blue curve show the annual mean (from July 2009 to June 2010), winter (December, January and February) and summer (June, July and August) vertical profile of NO_2 over Hong Kong obtanined from GEOS-Chem simulation. The magenta curve shows the a-priori vertical profile used in the OMI retrieval of NO_2 over Hong Kong.

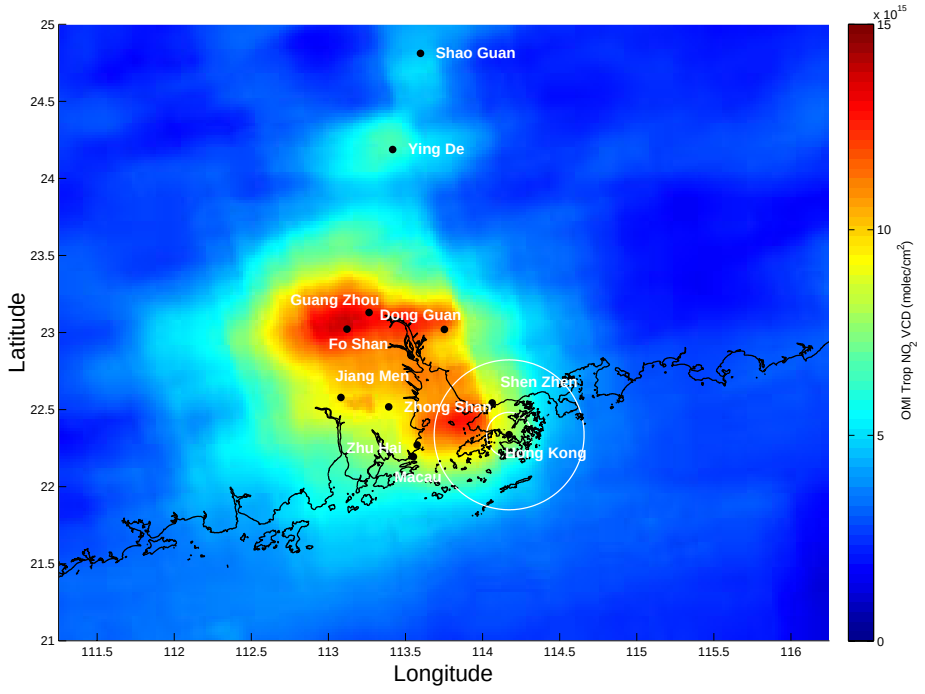

Fig. 7. Average OMI tropospheric NO_2 vertical column density gridded with a $0.02^\circ \times 0.02^\circ$ resolution over South China from December 2009 to March 2011. The two circles indicate the averaging area of the OMI data with Hong Kong in the centre.

of the NO_2 plume covering the entire Pearl River Delta which means increasing the averaging area to increase spatial coverage would include other sources not related to local emissions measured by the LP-DOAS. This agrees with the fact that the correlation coefficient decreases to 0.64 for the corresponding data sets. On average the monthly means of the OMI data within 15 km and 50 km are lower than the LP-DOAS measurement by 15.54 ppbv and 17.46 ppbv, respectively. To analyze the discrepancy, we compared different NO_2 vertical profiles for the tropospheric vertical columns to ground level mixing ratios conversion (see Figure 6). Using the annual mean profile (July 2009 to June 2010) from GEOS-Chem model runs, we found the conversion factor was about 2.12 times higher than the one for the OMI a-priori profile. Profiles from different seasons show about 10 % lower conversion factors in winter (December, January and February) and about 15 % higher conversion factors in summer (June, July and August). In order to investigate the effect of using these GEOS-Chem profiles from 2009/10 instead of the GEOS-Chem profiles from 1996/97 used in the OMI data product (see Figure 6) on the VCD retrieval we calculated new AMFs for Summer and Winter. The results show that the VCDs would be 14.8 % higher in Summer and 16.9 % higher in Winter. As the NO_x emissions over China has been reported to nearly doubled from 2000 to 2006

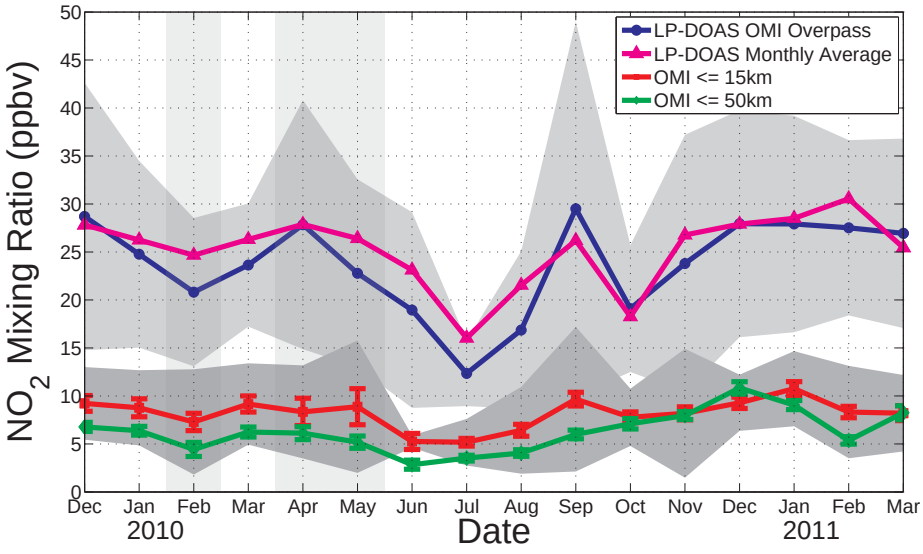

Fig. 8. Monthly mean ground level NO_2 mixing ratio. LP-DOAS data are temporal averages around OMI overpass times (blue curve). Monthly averages for all LP-DOAS data is shown for reference (magenta curve). OMI data are spatial averages over pixels within a 15 km (red curve) and 50 km (green curve) radius of the instrument. The light gray and gray regions indicate the variability (1 standard deviation) of LP-DOAS data during OMI overpass time and OMI data within a 15 km, respectively. The shadowed regions indicate months where OMI data are very sparse (less than 3 data points per month due to the cloud filtering).

(Zhang et al., 2007), this suggests that the a-priori profile used in the OMI retrieval might be out of date and causing underestimation.

The light gray and gray regions shown in Figure 8 represent the 1σ variability of the NO_2 mixing ratios within the months measured by the LP-DOAS and OMI, respectively, while the error bars of the OMI data represent the 1σ uncertainties of the OMI measurements. The error bars for the LP-DOAS measurements are too small to be shown. The averaged variability of the NO_2 mixing ratios in winter (December, January and February), spring (March, April and May), summer (June, July and August) and autumn (September, October and November) are 10.6 ppbv, 9.8 ppbv, 7.3 ppbv and 13.2 ppbv, respectively. The errors of the monthly OMI data are calculated by the standard error propagation and base on the assumption that all errors are randomly distributed. The error bars are larger for the months when only a small number of data points were available due to cloud filtering, e.g., February, April and May of 2010. In most of the months, the error bars of OMI data, either within 15 km or within 50 km, do not overlap with the LP-DOAS data, which indicated that there are some unknown systematic errors either in the OMI retrieval (Wenig et al., 2008) or the VCDs to ground level mixing ratios conversion, or both. One possible reason for the lower OMI values over Hong Kong compared to the LP-DOAS measurements is that the OMI a-priori profile used for

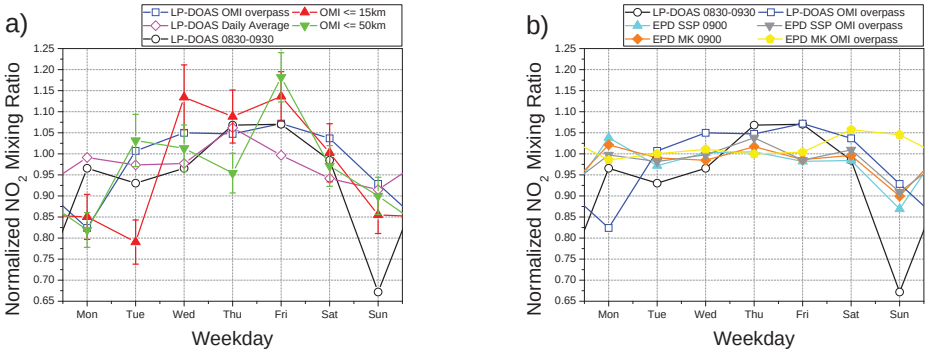

Fig. 9. Mean weekly cycle of NO_2 measured by LP-DOAS, OMI and EPD. (**a**) LP-DOAS data are temporal averages around OMI overpass time (blue curve), around the morning rush hour (black curve) and daily averages (magenta curves), OMI data are spatial averages within 15 km (red curve) and 50 km (green curve). (**b**) LP-DOAS data (black curve), EPD data from Sham Shui Po (cyan curve) and Mongkok (orange curve) monitoring station are temporal averages around the morning rush hour. OMI overpass time LP-DOAS data, EPD data from Sham Shui Po and Mongkok monitoring station are show as blue, gray and yellow curve, respectively. The values show on both plots are normalized with respect to the mean weekday (Monday to Friday) value (relative units). The error bars of the LP-DOAS and EPD data are not shown, since they are too small to be visible.

converting the tropospheric NO_2 VCDs to ground level mixing ratios is averaged over a large area around the Pearl River Delta Region including large fractions of ocean and rural area with lower relative ground level mixing ratio. Underestimation of the relative ground level mixing ratios in the conversion profile leads to underestimation of the ground level NO_2. Compared with the annually averaged profile form July 2009 till June 2010, the a-priori profile used in the OMI retrieval is causing underestimation of the VCDs by about 15 % and another 53 % during conversion to ground mixing ratios, resulting in an underestiation for the grounf level NO_2 of about 60 %.

3.3 Daily and Weekly Cycle of NO_2

Figure 9 shows the normalized mean weekly cycle of NO_2 for Hong Kong measured by the LP-DOAS, OMI and EPD. For each day of the week we calculated the mean of the LP-DOAS measurements, the OMI observations (cloud filtered) and EPD measurements for the entire LP-DOAS measurement period from December 2009 to March 2011. LP-DOAS data are temporal averages around OMI overpass time (13:30 to 14:30), OMI data are spatial averages within 15 km and 50 km. Temporal averages of the LP-DOAS data around the morning rush hour (08:30 to 09:30), and the entire day, as well as EPD data are shown for reference. Both datasets are normalized by the mean weekday (Monday to Friday) value for better comparison, and to emphasize the relative reduction of NO_2 mixing ratio on Sunday.

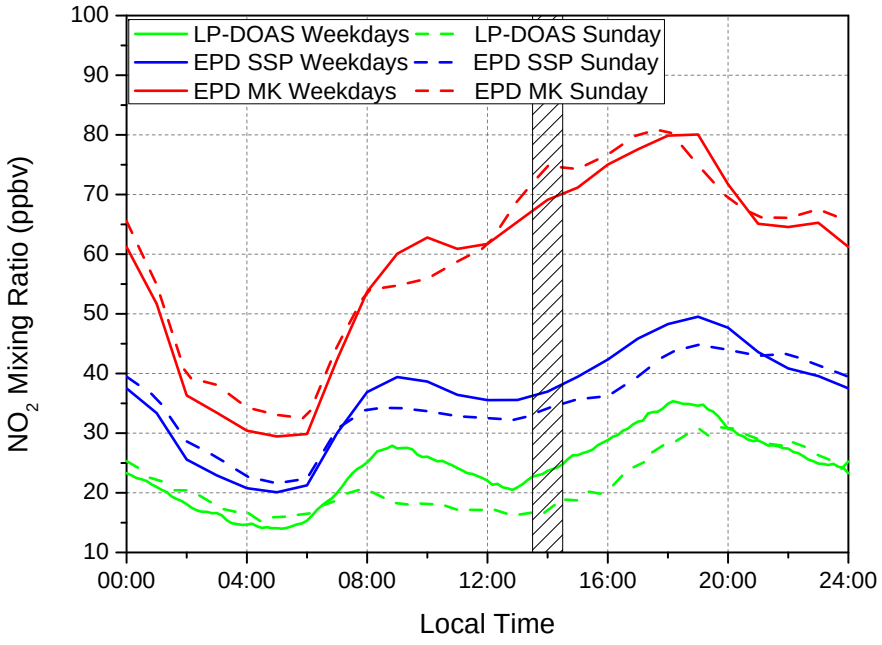

Fig. 10. Annual mean daily NO_2 cycle of the LP-DOAS, EPD Sham Shui Po and Mongkok measurements for weekdays and Sunday for data from December 2009 to November 2010. The green, blue and red curves indicate the mean daily NO_2 cycle for weekdays of the LP-DOAS, EPD Sham Shui Po and Mongkok measurements, respectively. The dashed green, blue and red curves indicate the mean daily NO_2 cycle for Sunday of the LP-DOAS, EPD Sham Shui Po and Mongkok measurements, respectively. The hatched region indicates the OMI overpass time for Hong Kong.

The OMI data and LP-DOAS data during OMI overpass agree with each other and show no significant weekly cycle. Our observation agrees with observations by Beirle et al. (2003) and Wenig (2001) that no significant NO_2 weekly cycle can be found over Hong Kong from space. However, such a cycle can be observed in the LP-DOAS measurements as well as the EPD data during the morning rush hour (08:30 to 09:30). The weekly cycle shows that the NO_2 level reduces by more than 30 % on Sundays compared to weekdays. Weekly cycles obtained by the EPD monitoring stations show a less pronounced reduction (about 15 %) on Sunday. This could be explained by the fact that both EPD stations are loacted in commercial area which are quite busy throughtout the whole week, while the LP-DOAS measurements cover both residential and commercial areas.

The mean daily cycles of NO_2 mixing ratios measured by the LP-DOAS, EPD Sham Shui and Mongkok monitoring stations for weekdays and Sunday are shown in Figure 10. The LP-DOAS measurements and the EPD data show similar characteristics with peaks in the morning and evening

rush hours. In general, NO_2 levels reach a minimum around 5:00 (local time) in the morning, followed by an increase from 5:00 to 9:00. The NO_2 levels decreases from 9:00 to 13:00 then it increases again and reaches the daily maximum around 18:00. The two peaks in the morning and the evening are due to an increase in traffic load during rush hours. Less traffic emissions and strong irradiance converting NO_2 to NO and ozone result in lower NO_2 levels at noon. The measured NO_2 is mainly due to traffic, as natural NO_2 emissions have no weekly and no strong diurnal cycle with typical much lower levels than observed. Power plant and industrial NO_2 emissions from the Pearl River Delta would be expected to show a distinct dependency on wind direction which could not be observed in our LP-DOAS measurements data.

From Figure 10, it is obvious that the daily NO_2 cycle for weekdays and Saturdays are almost the same. Most of the people in Hong Kong have to work on Saturdays, hence the traffic volume on Saturday is similar to that of weekdays. The NO_2 level reduces significantly on Sunday morning by more than 30 % compared to weekdays. It gradually returns to a weekday level in the afternoon. This pattern might be be explained by the fact that the majority of the population does not have to work on Sunday and go out in the afternoon.

Similar to the noon LP-DOAS data, OMI NO_2 observations do not show any reduction on Sunday. This suggests that satellite data with a single overpass per day are not sufficient to interpret weekly cycles of components which show a strong daily variability, empathizing the importance for geostationary satellite observation in this case.

4 Summary and Conclusion

In this paper, we described the instrumental setup and automatic data retrieval process of the LED based long path DOAS instrument running operationally at City University of Hong Kong since December 2009 in order to monitor surface air pollution conditions in Hong Kong. The measured NO_2 data show strong daily, weekly and seasonal variability. The annually averaged NO_2 mixing ratio is 23.5 ppbv but regularly exceeds 42.5 ppbv (Hong Kong air quality annual objective value). The NO_2 mixing ratios vary from 2.6 ppbv to 110.9 ppbv during the entire measuring period.

Our LP-DOAS measurements are compared to the NO_2 mixing ratio reported by a nearby monitoring station operated by the Hong Kong Environmental Protection Department (EPD). Hourly averages of coinciding measurements correlate well with a correlation coefficient R=0.71 for the 550 m absorption path and 0.79 for the 3820 m path. However, the EPD measurements show higher NO_2 mixing ratio than the LP-DOAS measurements by 11.5 ppbv for the shorter path (setup 1) and 15.6 ppbv for the longer path (setup 2). This discrepancy can be explained by different measurement heights and locations. Previous study reported that the chemiluminescence analyzers are likely to be overestimating the NO_2 levels due to cross interferences from other nitrogen compounds.

The LP-DOAS measurements during the OMI overpass time (13:30 - 14:30) are used to vali-

date OMI satellite NO_2 measurements over Hong Kong. Monthly averaged data of the LP-DOAS and OMI within 15 km radius of the LP-DOAS correlate well with a correlation coefficient of 0.84 and show that OMI measures reliable ground level NO_2. However, the OMI data are on average 15.54 ppbv lower than the LP-DOAS measurements. This discrepancy is mainly due to the a-priori NO_2 vertical profile used for the OMI retrieval and conversion of OMI NO_2 VCDs to ground level mixing ratios. By comparing the OMI a-priori profile to more up to date profiles shows the a-priori profile used in the OMI retrieval might be out of date and lead to an underestimation of the NO_2 level in Hong Kong.

Weekly cycles from OMI data and LP-DOAS data show clear differences. Daily NO_2 cycles from LP-DOAS measurements show significant peaks in the morning and evening rush hour due to increased traffic. The weekly cycle of NO_2 shows significant reduction on Sunday morning, but a typical weekday level for the rest of the day. This explains why OMI cannot observe a weekly cycle for Hong Kong, since the satellite's overpass time is around 14:00. We demonstrate that satellite data with a single overpass per day are not in general suitable to derive weekly cycles of compounds with strong diurnal variation.

Acknowledgements. The authors would like to thank Langham Place, Mongkok, Hong Kong for cooperating with CityU on this project and for the installation of the retro reflector at their building. The work described in this paper was partial supported by a grant from the Research Grants Council of the Hong Kong Special Administrative Region, China (Project No. CityU 102809), a grant from City University of Hong Kong (Project No. 7008077) and the German DAAD (Project No. PPP- D/09/00817).

References

Beirle, S., Platt, U., Wenig, M., and Wagner, T.: Weekly cycle of NO_2 by GOME measurements: a signature of anthropogenic sources, Atmos. Chem. Phys., 3, 2225–2232, DOI:10.5194/acp–3–2225–2003, 2003.

Bey, I., Jacob, D., Yantosca, R., Logan, J., Field, B., Fiore, A., Li, Q., Liu, H., Mickley, L., and Schultz, M.: Global modeling of tropospheric chemistry with assimilated meteorology: Model description and evaluation, J. Geophys. Res., 106, 23 073, DOI: 10.1029/2001JD000 807, 2001.

Boersma, K. F., Bucsela, E. J., Brinksma, E. J., and Gleason, J. F.: NO_2, OMI-EOS Algorithm Theoretical Basis Document: Trace Gas Algorithms: NO_2, 2001.

Bucsela, E., Celarier, E., Wenig, M., Gleason, J., Veefkind, P., Boersma, K., and Brinksma, E.: Algorithm for NO_2 vertical column retrieval from the Ozone Monitoring Instrument, IEEE Transactions on Geoscience and Remote Sensing, 44, 1245–1258, 2006.

Burrows, J. P., Richter, A., Dehn, A., Deters, B., Himmelmann, S., Voigt, S., and Orphal, J.: Atmospheric remote sensing reference data from GOME 2 Temperature-dependent absorption cross-sections of O_3 in the 231 V 794 nm range, J. Quant. Spectrosc. Radiat. Transfer, 61, 509–517, 1999.

Dunlea, E. J., Herndon, S. C., Nelson, D. D., Volkamer, R. M., San Martini, F., Sheehy, P. M., Zahniser, M. S., Shorter, J. H., Wormhoudt, J. C., Lamb, B. K., Allwine, E. J., Gaffney, J. S., Marley, N. A., Grutter, M., Marquez, C., Blanco, S., Cardenas, B., Retama, A., Ramos Villegas, C. R., Kolb, C. E., Molina, L. T., and Molina, M. J.: Evaluation of nitrogen dioxide chemiluminescence monitors in a polluted urban environment, Atmos. Chem. Phys., 7, 2691–2704, 2007.

Greenblatt, G., Orlando, J., Burkholder, J., and Ravishankara, A.: Absorption measurements of oxygen between 330 and 1140 nm, J. Geophys. Res., 95, 18 577–18 582, 1990.

Harder, J. W. and Brault, J. W.: Atmospheric measurements of water vapor in the 442nm region, J. Geophys. Res., 102, 6245–6252, 1997.

Kraus, S.: DOASIS A Framework Design for DOAS, Ph.D. thesis, Combined Faculties for Mathematics and for Computer Science, University of Mannheim, 2005.

Lau, J., Hung, W., Cheung, C., and Yuen, D.: Contributions of roadside vehicle emissions to general air quality in Hong Kong, Transportation Research Part D, 13, 19–26, 2008.

Lee, D. S., Köhler, I., Grobler, E., Rohrer, F., Sausen, R., Gallardo-Klenner, L., Olivier, J. G. J., Dentener, F. J., , and Bouwman, A.: Estimations of Global NO_x Emissions and Their Uncertainties, Atmos. Environ., 31, 1735–1749, 1997.

Levelt, P. F., van den Oord, G. H. J., Dobber, M. R., Malkki, A., Visser, H., de Vries, J., Stammes, P., Lundell, J. O. V., , and Saari, H.: The Ozone Monitoring Instrument, IEEE Trans. Geo. Rem. Sens., 44, 1093–1101, 2006.

Merten, A., Tschritter, J., and Platt, U.: New Design of DOAS-Long-path Telescopes based on fiber optics, Appl. Optics, 50, 783–754, 2011.

Palmer, P., Jacob, D., Chance, K., Martin, R., Spurr, R., Kurosu, T., I. Bey, R. Y., and Fiore, A.: Air mass factor formulation for spectroscopic measurements from satellites: Application to formaldehyde retrievals from the Global Ozone Monitoring Experiment, J. Geophys. Res., 106, 14 539–14 550, 2001.

Platt, U., Perner, D., and Patz, H.: Simultaneous measurement of atmospheric CH_2O, $O_3$and NO_2 by differential optical absorption, J. Geophys. Res., 84, 6329–6335, 1979.

Rothman, L., Barbe, A., Benner, D. C., Brown, L., Camy-Peyret, C., Carleer, M., Chance, K., Clerbaux, C., Dana, V., Devi, V., Fayt, A., Flaud, J.-M., Gamache, R., Goldman, A., Jacquemart, D., Jucks, K., Lafferty, W., Mandin, J.-Y., Massie, S., Nemtchinov, V., Newnham, D., Perrin, A., Rinsland, C., Schroeder, J., Smith, K., Smith, M., Tang, K., Toth, R., Auwera, J. V., Varanasi, P., and Yoshino, K.: The HITRAN molecular spectroscopic database: edition of 2000 including updates through 2001, J. Quant. Spectrosc. Radiat. Transfer, 82, 5–44, 2003.

Solomon, S., Schmeltekopf, A. L., and Sanders, R. W.: On the interpretation of zenith sky measurements, J. Geophys. Res., 92(D7), 8311–8319, 1987.

Solomon, S., Portmann, R. W., Sanders, R. W., Daniel, J. S., Madsen, W., Bartram, B., and Dutton, E. G.: On the role of nitrogen dioxide in the absorption of solar radiation, J. Geophys. Res., 104, 12 047–12 058, 1999.

Stutz, J. and Platt, U.: Numerical Analysis and Estimation of the Statistical Error of Differential Optical Absorption Spectroscopy Measurements with Least-Squares methods, Appl. Optics, 35, 6041–6053, 1996.

Stutz, J. and Platt, U.: Improving longpath differential optical absorption spectroscopy with a quartz-fiber mode mixer, Appl. Optics, 36, 1105–1115, 1997.

Vandaele, A. C., Hermans, C., Simon, P. C., Carleer, M., Colin, R., Fally, S., Merienne, M. F., Jenouvrier, A., and Coquart, B.: Measurements of the NO_2 absorption cross-section from 42000 cm^{-1} to 10000 cm^{-1} (238 - 1000 nm) at 220 K and 294 K, J. Quant. Spectrosc. Radiat. Transfer, 59, 171–184, 1998.

Voigt, S., Orphal, J., Bogumil, K., and Burrows, J. P.: The temperature dependence (203-293 K) of the absorption cross sections of O_3 in the 230-850 nm region measured by Fourier-transform spectroscopy, J. Photochem. Photobiol., 143, 1–9, 2001.

Voigt, S., Orphal, J., and Burrows, J. P.: The temperature and pressure dependence of the absorption cross-sections of NO_2 in the 250-800 nm region measured by Fourier-transform spectroscopy, J. Photochem. Photobiol., 149, 1–7, 2002.

Volkamer, R., Spietz, P., Burrows, J., and Platt, U.: High-resolution absorption cross-section of Glyoxal in the UV/vis and IR spectral ranges, J. Photochem. Photobiol., 172, 35. DOI: 10.1016/j.jphotochem.2004.11.011, 2005.

Wenig, M.: Satellite Measurement of Long-Term Global Tropospheric Trace Gas Distributions and Source Strengths - Algorithm Development and Data Analysis, Ph.D. thesis, University of Heidelberg, 2001.

Wenig, M. O., Cede, A. M., Bucsela, E. J., Celarier, E. A., Boersma, K. F., Veefkind, J. P., Brinksma, E. J., Gleason, J. F., and Herman, J. R.: Validation of OMI tropospheric NO_2 column densities using direct-sun mode Brewer measurements at NASA Goddard Space Flight Center, J. Geophys. Res., 133, D16S45, DOI:10.1029/2007JD008 988, 2008.

Zhang, Q., Streets, D. G., He, K., Wang, Y., Richter, A., Burrows, J. P., Uno, I., Jang, C. J., Chen, D., Yao, Z., and Lei, Y.: NO_x emission trends for China, 1995-2004: The view from the ground and the view from space, J. Geophys. Res., 112, D22 306, DOI:10.1029/2007JD008 684, 2007.